

Nernst effect in $\text{NdBa}_2\{\text{Cu}_{1-y}\text{Ni}_y\}_3\text{O}_{7-\delta}$ ($y=0-0.12$)

N. Johannsen,^{1,*} Th. Wolf,² A. V. Sologubenko,¹ T. Lorenz,¹ A. Freimuth,¹ and J. A. Mydosh¹

¹*II. Physikalisches Institut, Universität zu Köln, Zùlpicher Strasse 77, 50937 Köln, Germany*

²*Forschungszentrum Karlsruhe, Institut für Festkörperphysik, 76021 Karlsruhe, Germany*

(Received 13 April 2007; revised manuscript received 8 June 2007; published 26 July 2007)

In $\text{NdBa}_2\{\text{Cu}_{1-y}\text{Ni}_y\}_3\text{O}_{7-\delta}$ magnetic Ni-impurities suppress T_c but at the same time the pseudogap is strongly enhanced. This unique feature makes it an ideal system to study possible relations between the anomalous Nernst effect, superconductivity, and the pseudogap. We present Nernst effect measurements on a series of optimally doped (O_7) and underdoped ($\text{O}_{6.8}$) samples with Ni contents ranging from $y=0$ to 0.12. In all samples an onset of the Nernst signal is found at $T^N > T_c$. For the optimally doped samples T^N and T_c decrease simultaneously with increasing Ni content. The underdoped samples show a different behavior, i.e., the onset of the Nernst signal is hardly affected by increasing the Ni content from $y=0$ to 0.03. Irrespective of the oxygen content, T^N clearly does not track the enhanced pseudogap temperature T^* .

DOI: 10.1103/PhysRevB.76.020512

PACS number(s): 74.40.+k, 72.15.Jf, 74.62.Dh, 74.72.-h

More than 20 years after the discovery of high-temperature superconductivity the pairing mechanism is still unsolved. Possible relations to other anomalous phenomena in high- T_c materials such as the pseudogap phase may play a key role towards an understanding of this mechanism. The pseudogap is exhibited in the normal-state region of the underdoped compounds. The first evidence for a pseudogap in the charge channel was reported on the basis of optical conductivity data,¹ extending to temperatures $T^* \gg T_c$. It has been suggested that this phenomenon is related to superconductivity via preformed Cooper pairs that are thermally prevented from forming long-range phase coherence.² Other suggestions include novel phases that may even compete with superconductivity, such as exotic spin or charge density wave states³⁻⁶ and stripe ordering scenarios.⁷ The preformed-pair scenario seems to be the most attractive description because it corresponds to the three-dimensional equivalent of the well-known two-dimensional Kosterlitz-Thouless (KT) transition in which thermally excited vortices (in zero field) destroy phase rigidity but not the pairing amplitude.

Anomalous Nernst signals that are detectable far into the pseudogap region as well as a diamagnetic response which scales with the Nernst effect support this description.⁸ Since a large Nernst effect in the mixed state of type-II superconductors is attributed to moving vortices⁹ it is a very accurate probe for vortex formation and vortexlike excitations. The Nernst signal is anomalous if it extends into the normal-state region because a charge carrier Nernst signal is usually very small in normal metals due to the so-called “Sondheimer cancellation.”¹⁰ In clean high- T_c 's with moderate inelastic scattering the carrier-Nernst signal can reach values of about 25% of the magnitude of the vortex-Nernst signal but it is linear in field and opposite in sign to the vortex signal.¹¹ Thus it is obvious that Nernst effect measurements can effectively contribute to unravel and clarify the pseudogap phenomena.

In order to facilitate such investigations one should examine a system in which the most relevant parameters, T_c and T^* , can be tuned individually. Given such a system, one could examine the properties of the anomalously enhanced Nernst signals that are found above T_c and below T^* . In order to determine if there is a connection to the pseudogap, one

just has to shift the pseudogap and observe whether the Nernst signal follows or not. Fortunately, such a system exists, namely $\text{NdBa}_2\{\text{Cu}_{1-y}\text{Ni}_y\}_3\text{O}_{7-\delta}$. Recent measurements of the optical conductivity of Ni-doped $\text{NdBa}_2\text{Cu}_3\text{O}_{7-\delta}$ revealed a strongly enhanced pseudogap while superconductivity is suppressed at the same time.¹² This compound therefore offers the unique opportunity to study the development of the Nernst signal while tuning T_c and the pseudogap individually and even in opposite directions. Our measurements were performed on a series of optimally doped (O_7) and underdoped ($\text{O}_{6.8}$) samples with Ni contents ranging from $y=0$ to 0.12. Irrespective of the oxygen content, the onset of the Nernst signal (T^N) clearly does not follow the enhanced pseudogap.

The high-quality single crystals of $\text{NdBa}_2\{\text{Cu}_{1-y}\text{Ni}_y\}_3\text{O}_{7-\delta}$ used in our study were grown by a flux method as described in detail in Ref. 12. Ni substitution does not alter the hole doping content significantly which is confirmed by thermopower measurements. It is estimated that half of the Ni impurities reside within the CuO_2 planes. The influence of substituting magnetic Ni ions or nonmagnetic Zn ions in the CuO_2 planes has been investigated by several groups.¹³⁻¹⁵ In $\text{YBa}_2\text{Cu}_3\text{O}_{7-\delta}$ (YBCO) a linear depression of T_c is found for both impurities.¹³ STM measurements revealed the local electronic structure for both substitutes.¹⁴ Ni retains a local magnetic moment and the superconducting energy gap is unimpaired. Scattering at this site is then mostly determined by potential interactions. The effects of impurity doping on the onset of the Nernst effect has been studied by several groups. In Zn-doped $\text{YBa}_2\text{Cu}_3\text{O}_7$ T^N was found to decrease with T_c while the pseudogap is left untouched.¹⁵ In electron irradiated samples of $\text{YBa}_2\text{Cu}_3\text{O}_7$ and $\text{YBa}_2\text{Cu}_3\text{O}_{6.6}$ a constant onset of the Nernst effect was reported for both samples,¹⁶ but the authors did not address the relation between the Nernst effect and the pseudogap. Depending on the Ni-impurity level in $\text{NdBa}_2\{\text{Cu}_{1-y}\text{Ni}_y\}_3\text{O}_{7-\delta}$, we can compare the enhanced pseudogap to T_c and T^N .

The Nernst effect measurements were carried out on four optimally doped $\text{NdBa}_2\{\text{Cu}_{1-y}\text{Ni}_y\}_3\text{O}_7$ samples. The T_c values and transition width ΔT_c are taken as the midpoint of the diamagnetic transition and the 10%–90% width of the tran-

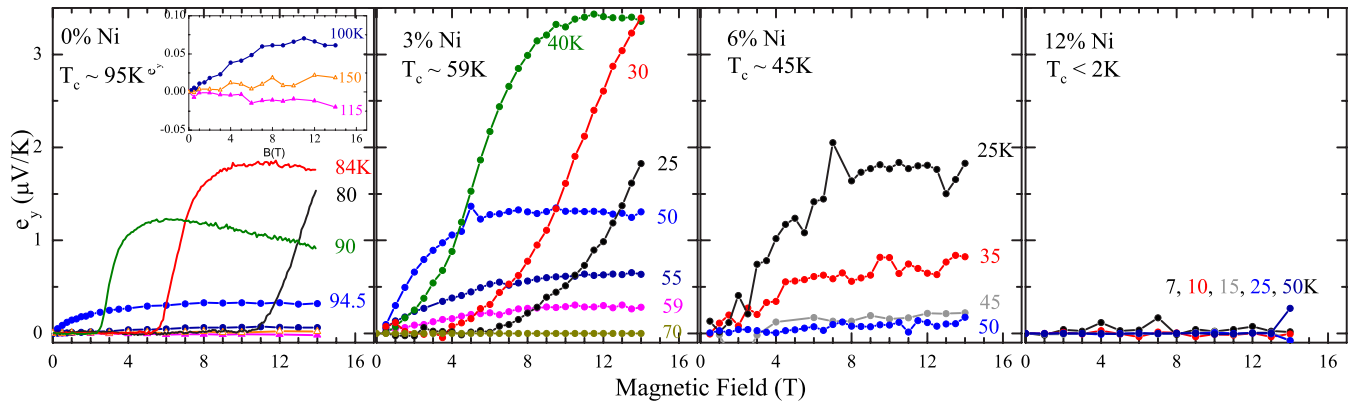


FIG. 1. (Color online) Typical Nernst signals of a series of optimally doped $\text{NdBa}_2\{\text{Cu}_{1-y}\text{Ni}_y\}_3\text{O}_7$. The inset enlarges the contributions to the Nernst signal above T_c .

sition, respectively. A pure sample with $T_c=95(\Delta T_c=1)$ K, and three samples with $y=0.03$ [$T_c=59(8)$ K], 0.06 [$T_c=45(10)$ K], and 0.12 with $T_c<2$ K were used. By annealing in flowing O_2 atmosphere at about 540°C and $p=1$ bar a series of underdoped ($\text{O}_{6.8}$) samples were prepared: $y=0$ [$T_c=53(7)$ K], 0.03 [$T_c=20(14)$ K], and 0.06 with $T_c<2$ K. Typical sample sizes were $1\times 1\times 0.5\text{ mm}^3$. For the Nernst effect measurements two thin copper wires were attached at the sides of the sample with a two-component silver epoxy in order to pick up a transverse voltage. The sample was then mounted to a copper block which was at the same temperature as the temperature-stabilized surrounding. On the top of the sample a chip heater was thermally connected by an insulating varnish (VGE 7031, Lakeshore). By applying power to the heater a temperature gradient is created over the sample of about 0.5 K/mm which is detected by a AuFe-Chromel thermocouple. Two methods were used to detect the Nernst signals. Most of the measurements were performed by stabilizing the temperature (to about 1 mK) and the temperature gradient for each magnetic field (typically in steps of 0.5 T). Then the temperature gradient is removed in order to subtract offset voltages. For the second method the temperature is stabilized again very accurately (1 mK), then the heater power is switched on and the field is continuously swept at a typical rate of about 0.3 T/min . A second sweep with the heater switched off is performed at the same temperature in order to remove field-dependent offset voltages. Both methods give excellent agreement. The Nernst signal itself is extracted as the anti-symmetric part of the field-dependent transverse voltages in order to eliminate thermopower voltages due to possible misalignments of the contacts and is given by

$$e_y = \nu B_z = \frac{E_y}{-\nabla T_x}, \quad (1)$$

where ν is the Nernst coefficient and E denotes the electric field.

Figure 1 shows measurements of the optimally doped samples for Ni contents of 0%, 3%, 6%, and 12%. At low T , the signal is zero until a typical temperature-dependent melting field is reached. At that field the density of vortices is

sufficiently high to overcome pinning forces. In the adjacent “vortex-liquid” phase the vortices are free to move towards the cold end of the sample and thereby are able to produce the phase-slip voltage that gives the anomalously enhanced Nernst signal. This causes the steep increase in the Nernst signal. When the field is further increased, the signal saturates until it slowly diminishes towards the upper critical field H_{c2} . This results in the characteristic “tilted-hill” profile of the Nernst signal in high- T_c cuprate superconductors.¹⁷ Now increasing the temperature and approaching T_c the melting field begins to weaken until the signal rises immediately at $H=0$. Above T_c the signal drops very sharply until it becomes very small, negative, and linear in field.

The linear and negative contribution in the normal state that can be identified with the quasiparticle (QP) background^{11,18} is very small in this optimally doped compound. This small background seems to be a common feature of the optimally doped $[\text{Y,Nd}]\text{-BCO}$ samples,^{8,15,16} independent of the impurity content. Increasing the Ni content to 3%, the absolute values of the signals increase while T_c drops to $59(8)$ K. In contrast to the sharp increase of the signal after exceeding the melting field in the pure sample, the signal rises more smoothly in the 3% Ni-doped compound. By further increasing the Ni content to 6% the absolute values of the Nernst signal decrease again until the sig-

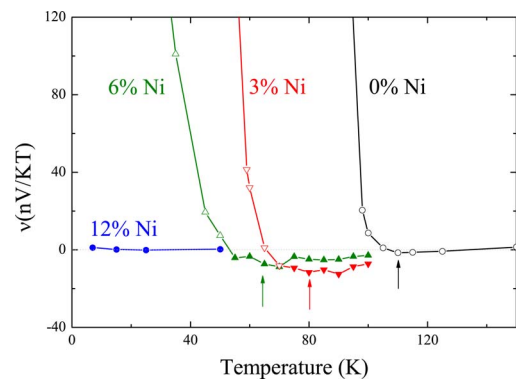


FIG. 2. (Color online) Nernst coefficients ν versus temperature for the pure and three Ni-doped (O_7) single crystals (Ref. 19). Onset temperatures are indicated by arrows.

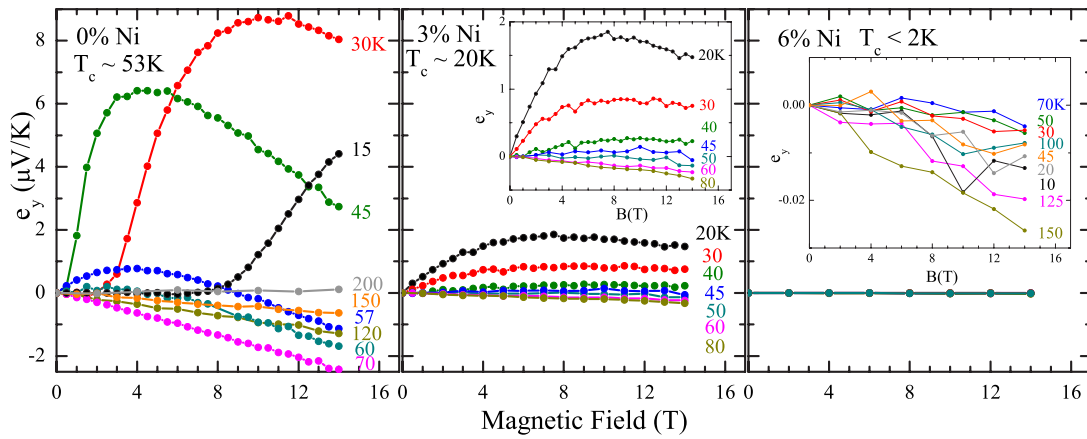


FIG. 3. (Color online) Nernst signal of a series of underdoped $\text{NdBa}_2\{\text{Cu}_{1-y}\text{Ni}_y\}_3\text{O}_{6.8}$. The insets show an expanded view of the data.

nal cannot be distinguished from the background at 12% Ni. In the entire series of the optimally doped samples the Nernst signal above T_c drops quickly. As mentioned above the QP contribution is very small.

Figure 2 shows the Nernst coefficient, $\nu = e_y/B_z$. Dividing by the field yields a field independent value only for the linear contributions of the Nernst signals produced by the QP background. At lower T , a voltage due to vortex movement adds to the QP contribution which leads to a strong field dependence of $\nu = \nu(B)$. In Fig. 2 the open symbols are derived by linearly fitting the initial slope of e_y .¹⁹ The onset of the Nernst signal is then defined as the most negative value of ν . In Ref. 12 it is reported that the pseudogap can be restored or even enhanced by adding Ni-impurities to the optimally doped (or slightly overdoped) samples. This enhanced pseudogap can now be compared to the onset of the Nernst signals. The onset, T^ν of Fig. 2 (indicated by arrows), shifts to lower temperatures as the Ni content is increased. If there was a scaling of T^ν with the pseudogap temperature one would expect the opposite behavior since the sample with 12% Ni is identified with the highest pseudogap temperature.¹² Here the decrease of T^ν is, however, closely connected to the decrease of T_c .

Next, we consider the behavior of the underdoped compounds at Ni-impurity levels of 0%, 3%, and 6% (Fig. 3).

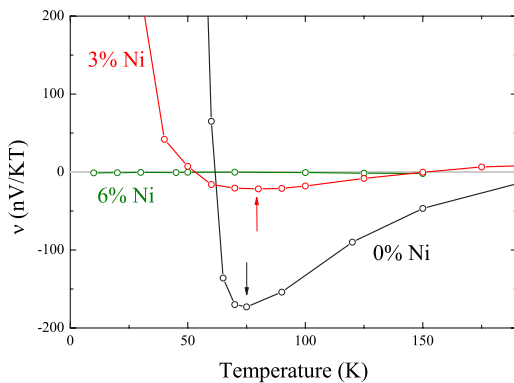


FIG. 4. (Color online) Nernst coefficients ν of the underdoped compounds (onset temperatures are marked by arrows).

The pure sample shows the largest vortex contribution to the Nernst signal of all measured samples. In addition, a very large negative QP signal is present which exceeds $-2 \mu\text{V/K}$ at 70 K and 14 T. Adding Ni, the anomalous Nernst signal as well as the QP contribution decrease very sharply (3%) until the signal is further diminished and no systematic temperature dependence of the negative background can be deduced (6%). Surprisingly, the onset temperatures of both underdoped samples do not change with the Ni content (Fig. 4). This result differs from the onsets of the optimally doped series. All onset temperatures of our samples are collected in Fig. 5 as a function of T_c . These onsets can now be compared to the pseudogap data of Ref. 12. The fluctuation regime is found to be narrow in our pure samples, e.g., the onsets are determined to be about 20 K higher than T_c . The scaling behavior of T^ν changes from the O_7 to the $\text{O}_{6.8}$ compounds. Although T^ν of the optimally doped samples clearly follows T_c , the onsets of the underdoped ones seem to be independent of the Ni content; but clearly no scaling to the reported enhanced pseudogap can be established for both series since it is shown that the pseudogap and the pseudogap temperature increase with increasing Ni content.¹² Another criterion is the temperature which matches a slightly positive Nernst

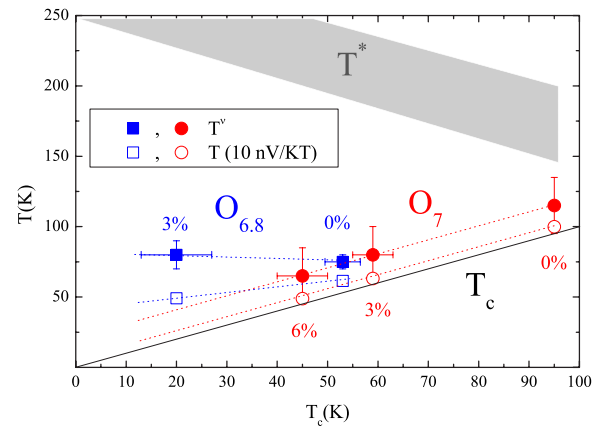


FIG. 5. (Color online) Onset temperatures of all samples versus T_c . The T^* band sketches the pseudogap opening temperatures as estimated from the results of Ref. 12.

coefficient of $\nu=10$ nV/KT.^{8,16} $T(\nu=10$ nV/KT) (open circles) scales downward from T^ν and is thereby proportional to T_c in the optimally doped compounds. The underdoped compounds develop a slope $T(\nu=10$ nV/KT) that tilts towards the slope of T_c (open squares) but is still clearly distinguishable from the optimally doped ones.

A sharp decay of the Nernst signal above T_c is predicted by Ref. 20 whose calculations yield a proportionality $T^\nu \sim T_c$. This result is in agreement with our findings from the optimally doped samples. The high onset with respect to T_c in the underdoped phase (3% Ni) is comparable to the high onsets found in electron-irradiated YBCO_{6.6} samples¹⁶ as well as in Y_{1-x}Pr_xBa₂Cu₃O_{7- δ} .²¹ These can be interpreted in terms of an unchanged T^ν while T_c is suppressed due to the impurity-induced disorder. Recent calculations connect the onset of the Nernst signal to the onset of superconductivity in spatially disordered systems.²² This onset is then

found to be at temperatures that represent the onset of superconducting islands, which percolate at T_c . This implies $T^\nu \ll T^*$, which coincides with our findings.

In summary, we have studied the Nernst effect for a series of optimally doped and underdoped NdBa₂{Cu_{1-y}Ni_y}₃O_{7- δ} samples with Ni concentrations varying between $y=0$ and 0.12. Substituting Ni for Cu gives the unique opportunity to study the development of the Nernst effect in a system where the pseudogap temperature T^* and the superconducting T_c can be tuned separately. For the optimally doped samples a clear scaling ($T^\nu \sim 20$ K + T_c) exists while in the underdoped ones T^ν remains Ni-independent. For both series, there is no correlation of T^ν with the enhanced pseudogap.

We acknowledge fruitful discussions with M. Vojta and D. I. Khomskii. This work was supported by the Deutsche Forschungsgemeinschaft through SFB 608.

*johannse@ph2.uni-koeln.de

¹C. C. Homes, T. Timusk, R. Liang, D. A. Bonn, and W. N. Hardy, Phys. Rev. Lett. **71**, 1645 (1993).

²V. J. Emery and S. A. Kivelson, Nature (London) **374**, 434 (1995).

³A. V. Chubukov and J. Schmalian, Phys. Rev. B **57**, R11085 (1998).

⁴I. Affleck and J. B. Marston, Phys. Rev. B **37**, 3774 (1988).

⁵X. G. Wen and P. A. Lee, Phys. Rev. Lett. **76**, 503 (1996).

⁶S. Chakravarty, R. B. Laughlin, D. K. Morr, and C. Nayak, Phys. Rev. B **63**, 094503 (2001).

⁷U. Löw, V. J. Emery, K. Fabricius, and S. A. Kivelson, Phys. Rev. Lett. **72**, 1918 (1994).

⁸Y. Wang, L. Li, and N. P. Ong, Phys. Rev. B **73**, 024510 (2006).

⁹Z. A. Xu, N. P. Ong, Y. Wang, T. Kakeshita, and S. Uchida, Nature (London) **406**, 486 (2000).

¹⁰E. H. Sondheimer, Proc. R. Soc. London, Ser. A **193**, 484 (1948).

¹¹V. Oganesyan and I. Ussishkin, Phys. Rev. B **70**, 054503 (2004).

¹²A. V. Pimenov, A. V. Boris, L. Yu, V. Hinkov, T. Wolf, J. L. Tallon, B. Keimer, and C. Bernhard, Phys. Rev. Lett. **94**,

227003 (2005).

¹³Y. K. Kuo, C. W. Schneider, M. J. Skove, M. V. Nevitt, G. X. Tessema, and J. J. McGee, Phys. Rev. B **56**, 6201 (1997).

¹⁴E. W. Hudson, K. M. Lang, V. Madhavan, S. H. Pan, H. Eisaki, S. Uchida, and J. C. Davis, Nature (London) **411**, 920 (2001).

¹⁵Z. A. Xu, J. Q. Shen, S. R. Zhao, Y. J. Zhang, and C. K. Ong, Phys. Rev. B **72**, 144527 (2005).

¹⁶F. Rullier-Albenque, R. Tourbot, H. Alloul, P. Lejay, D. Colson, and A. Forget, Phys. Rev. Lett. **96**, 067002 (2006).

¹⁷Y. Y. Wang, S. Ono, Y. Onose, G. Gu, Y. Ando, Y. Tokura, S. Uchida, and N. P. Ong, Science **299**, 86 (2003).

¹⁸Y. Y. Wang, Z. A. Xu, T. Kakeshita, S. Uchida, S. Ono, Y. Ando, and N. P. Ong, Phys. Rev. B **64**, 224519 (2001).

¹⁹Closed symbols represent values derived from $\nu=e_y(14T)/B$.

²⁰D. Podolsky, S. Raghu, and A. Vishwanath, arXiv:cond-mat/0612096 (unpublished).

²¹P. Li, S. Mandal, R. C. Budhani, and R. L. Greene, Phys. Rev. B **75**, 184509 (2007).

²²D. N. Dias, E. S. Caixeiro, and E. V. L. de Mello, arXiv:cond-mat/0607075 (unpublished).